Ethanol internal steam reforming in intermediate temperature solid oxide fuel cells

Stefan Diethelm* **and Jan Van herle**
Ecole Polytechnique Fédérale de Lausanne (EPFL)
Industrial Energy System Laboratory (LENI)
STI-IGM-LENI
ME A2 435
Station 9
CH-1015 Lausanne
Tel.: +41-21-693-5357
Fax: +41-21-693-3502
Stefan.diethelm@epfl.ch

Abstract

This study investigates the performance of a standard Ni-YSZ anode supported cell under ethanol steam reforming operating conditions. Therefore, the fuel cell was directly operated with a steam/ethanol mixture (3 to 1 molar). Other gas mixtures were also used for comparison to check the conversion of ethanol and of reformate gases (H_2, CO) in the fuel cell. The electrochemical properties of the fuel cell fed with 4 different fuel compositions were characterized between 710 and 860°C by I-V and EIS measurements at OCV and under polarization. In order to elucidate the limiting processes, impedance spectra obtained with different gas compositions were compared using the derivative of the real part of the impedance with respect of the natural logarithm of the frequency.

Results show that internal steam reforming of ethanol takes place significantly on Ni-YSZ anode only above 760°C. Comparisons of results obtained with reformate gas showed that the electrochemical cell performance is dominated by the conversion of hydrogen. The conversion of CO also occurs either directly or indirectly through the water-gas shift reaction but has a significant impact on the electrochemical performance only above 760°C.

Keywords: SOFC; Ni-YSZ anode; ethanol, internal reforming; coking; impedance spectroscopy

* Corresponding author

Introduction

Ethanol is considered as a valuable candidate fuel for SOFC application [1]. It offers many advantages: 1) Being a liquid, it has a high energetic density, it is easy to store, handle and transport; 2) As ethanol contains oxygen and is perfectly miscible with water, it can easily be reformed by steam without additional fuel processing; 3) ethanol is widely available and can be produced from renewable sources (agricultural byproducts, biomass) allowing for CO_2-neutral power generation.

Ethanol cannot be fed directly to standard SOFC with Ni-cermet anodes because of the problem of carbon deposition that de-activates the anode catalyst [2, 3]. This problem can be overcome either by adding water, which will help reforming the ethanol into H_2, CO and CH_4 that in turn can be directly converted in the SOFC or by developing new anode materials, inactive towards C-deposition [4-10].

SOFC technology is particularly adapted to internal steam reforming of ethanol because of the suitable operation temperatures (700-800°C) and the tolerance towards CO, requiring no additional conversion steps (WGS, PrOx). In addition, internal steam reforming of ethanol is particularly interesting from a heat management point of view because, being endothermic, it allows removing the extra heat produced within the stack without the need for a large air excess. On the system level, it also allows to economize on an external reformer.

There are several studies dedicated to the performance of SOFC fuelled with a mixture of water and ethanol [2, 11-19]. The first results were obtained with standard anode Ni-cermets, either as electrolyte supported cells [14] or as planar [12] and tubular [2] anode supported cells, all of them with small active areas (≤ 1 cm^2). Jiang and co-workers obtained power densities of 0.3 Wcm^{-2} at 650°C and 0.8 Wcm^{-2} at 800°C with a volumic

ratio of 1 on anode supported cells [12]. However, analysis of the gas outlet showed that in situ reforming did not readily occur at 800°C. The problem of carbon deposition was not addressed. Sasaki et al. obtained 0.3 Wcm^{-2} at 1000°C with an electrolyte supported cell [14]. There again, comparison of performances between internal and external steam reforming of ethanol showed that the conversion in a standard anode was not sufficient.

More recent papers examined the use of alternative anodes for direct internal steam reforming. Ye and co-workers studied a Cu-CeO_2-ScSZ composite, replacing Ni with Cu for current collection (Cu being less active for hydrocarbon cracking than Ni) and CeO_2 for the ethanol steam reforming (ESR) catalysis [15]. Power densities of 0.2-0.25 Wcm^{-2} were reached at 800°C for a water/EtOH volumic ratio of 2, which corresponds to the values obtained with H_2 at 750°C. However, as neither the local temperature nor the outlet composition were measured, an explanation of this difference was not possible. Short-term (50h) steady state operation was stable, but the issue of C-deposition was not closely investigated. A similar anode composition was also considered for other liquid fuels [20]. Huang et al. have studied the oxide anode (La,Sr)(Cr,Mn)O_3 with a La-gallate electrolyte [13]. As expected with such anode materials, the electro-chemical performances were poor (0.1 Wcm^{-2} at 800°C, H_2O/EtOH = 2 by vol.). Stability was demonstrated over 60h at 750°C and 60 $mAcm^{-2}$. The same author also investigated the use of Fe-Ni/ScSZ cermets prepared by impregnation of a porous SCSZ layer [11]. Only the Ni-free composition showed no C-deposit after 48h at 700°C with EtOH (EtOH:H2O=2:1 by vol.). The electrochemical performance of $Fe_{0.5}Ni_{0.5}$/ScSZ ASC was 20% lower than for Ni/ScSZ (0.5 Wcm^{-2} at 800°C). Both compositions activated during 48h polarization at 700°C with ethanol, despite C-deposition. This was attributed to an improvement of the electrical conductivity of the anode thanks to carbon.

In this paper, we investigate further internal steam reforming of ethanol on a standard Ni-YSZ anode-supported cell at intermediate temperatures (700-850°C). By comparing the

performance of the fuel cell fed with steam/ethanol (molar ratio 3 to 1) and its corresponding reformate, we try to identify the appropriate operating conditions and elucidate the limitations and underlying mechanisms of internal reforming. Other gas mixtures were also used to check the influence of steam and CO/CO_2. In addition, catalytic tests for ethanol steam reforming were conducted on ground Ni-YSZ anode for comparison with the electrochemical data.

1. Experimental

Catalytic tests

For the catalytic testing, a standard Ni-YSZ anode supported cell provided by HTceramix was ground in a mortar and sieved to obtain particle sizes comprised between 80 and 160 μm. 60 mg of the powder was packed between two quartz wool plugs inside a 4mm internal diameter quartz tube (cf. inset of Figure 1) placed in the centre of a furnace. The temperature of the reactor was measured with a K-type thermo-couple, protected by a quartz sleeve and positioned into contact with the catalytic bed. A schematic view of the set-up is depicted in Figure 1. A 10 $\mu l \cdot min^{-1}$ flow of 3:1 molar water:ethanol mixture was vaporized in a heated metal frit and diluted with 100 $Nml \cdot min^{-1}$ Ar before entering the reactor. The corresponding weight hourly space velocity (WHSV) was approximatively 2.5 $l_{etOH} g_{cat}^{-1} h^{-1}$.The composition of the product gas was analyzed with a gas chromatograph (GC, Varian), equipped with MS 5Å and Poraplot Q capillary columns coupled with TCD and FID detectors. The hot product gas was either directly fed to the GC for the quantification of ethanol and acetaldehyde vapors (a) or cooled down to condensate all vapors before the analysis of the permanent gases (b).

The catalyst was initially reduced at 950°C with 10% H_2 diluted in Ar. Measurements were performed starting at high temperature then lowering it gradually down to 500°C.

Electrochemical tests

The cell used in this study is a standard Ni-YSZ anode supported cell with a composite $(La_{0.70}Sr_{0.30})_{0.90}MnO_{3\pm\delta}$-8YSZ cathode (50% vol.) prepared by mixing the LSM powder (Fuel Cells Materials, USA) with ground 8YSZ powder (Tosoh Corp., Japan), both having an average particle diameter equal to 0.3 μm [21]. The cathode (∅ 12mm) was screen-printed on an anode supported electrolyte (∅ 20mm) provided by HTceramix (Switzerland). The applied ink consisted of 60 %wt powder, ethylcellulose binder and terpineol-based solvent.

The cathode was sintered in air at 1060°C for 1 hour. For the current collection, gold meshes (∅ 12mm) were contacted to the electrodes using $(La_{0.65}Sr_{0.35})_{0.95}MnO_{3\pm\delta}$ (Fuel Cells Materials, USA) paste on the cathode side and NiO (J.T. Baker)-8YSZ (90:10 %wt) on the anode side, sintered 1 hour at 1010°C.

The cell was assembled in a Probostat™ set-up (NorECs, Norway), as depicted in Figure 2: the cell was clamped between a bottom alumina tube and a spring loaded compression system. The gas tightness was achieved with a gold ring. The temperature was measured with a S-type thermocouple placed next to the cell (cf. Figure 2). Air was fed from the bottom by an internal tube and the fuel was brought to the anode via a quartz tube cane. The water (deionized) and the water/ethanol (99.8% Sigma-Aldrich) mixture was injected using a peristaltic pump (Ismatec, Switzerland) and vaporized through a heated metal frit.

The air flow was maintained at 100 $Nml \cdot min^{-1}$ throughout the test. The total fuel flow was kept at 50 $Nml \cdot min^{-1}$ but with three different compositions, which are given in Table 1. The “syngas” corresponds to the thermodynamic equilibrium composition of a 3 to 1 molar steam/ethanol reformed mixture. The minor (<2%) amount of CH_4 normally present at

lower temperature was ignored. In the “humid” mixture the CO and CO_2 were replaced by Ar, whereas in the “dry” mixture solely H_2 was maintained beside Ar. These gas mixtures are referred to hereafter by their name or their initial letter (**d**ry, **h**umid, **s**yngas). These different gas mixtures were used to check the influence of the different gas components on the performance of the Ni-YSZ anode. 32 $\mu l \cdot min^{-1}$ of liquid water/ethanol (3 to 1 molar) mixture was also vaporized and directly injected to the anode. This mixture is simply referred to as **e**tOH.

All electrochemical measurements (EIS, I-V) were performed with a IM6 electrochemical workstation (Zahner, Germany) using a two electrodes configuration with four wires. The I-V measurements were done in potentiostatic control mode from OCV to 0.6 V using 2 mVs^{-1} scans. All EIS measurements were performed with a 10 mV perturbation in the frequency range from 100 k to 0.1 Hz, under various current biases (OCV, 88, 265 and 442 $mAcm^{-2}$).

2. Results and discussion

Catalysis

The results for ethanol steam reforming on ground Ni-YSZ are shown in Figure 3. It can be observed that ethanol conversion is only 30% at 700°C but then rapidly increases to reach 80% at 780°C. Complete conversion occurs above 900°C. The gas composition after condensation of the vapors is also given in the same figure. The composition is very different from that predicted by thermodynamics (cf. Figure 4): in particular, the proportion of methane is more important above 780°C. Additionally, there is a significant amount of ethene (ethylene). The latter is usually produced by the dehydration of ethanol and provokes coke deposition through its decomposition.

Electrochemistry

All I-V curves obtained for the different gas compositions and temperatures are shown in Figures 5 to 8. The corresponding power densities measured at 0.7 V are plotted in Figure 9. Furthermore, the OCV measured with the humid and the etOH mixtures are compared in Table 2 with those calculated from thermodynamics using Nernst law. A few general observations can be drawn from these figures:

i) At 710°C, the performance of the fuel cell fed with a mixture of steam and ethanol is lower than with the corresponding syngas mixture, indicating that ethanol is not fully converted by the standard Ni-YSZ anode. This is however not the case above 760°C where the cell performance with ethanol even surpasses that obtained with syngas. These results can be understood in the light of the catalytic test performed on the ground Ni-YSZ anode support and reported above (cf. Figure 3): the cell performance is related to the availability of H_2 and therefore to the catalytic conversion of ethanol in the anode. At 700°C, the latter is only 30% whereas at 780°C it reaches 80%.

ii) Furthermore, at lower temperatures (< 760°C), the performances with the humid gas mixture and the syngas seem to coincide, indicating that H_2 is preferably converted electrochemically on Ni-YSZ than CO, which almost acts as an inert gas. The contribution of CO only becomes more significant at higher temperatures.

iii) Finally, at all temperatures, the presence of 20% excess steam in the fuel induces a cell voltage penalty clearly noticeable at open circuit. However, as the current density (i.e. the fuel utilization) increases, the difference between the I-V curves for the dry and humid gas mixtures vanishes.

In what follows, we shall look more carefully at the difference of performance between the different fuels by comparing the corresponding electrochemical impedance spectra. We hereby apply the method suggested by S.H. Jensen and co-workers [22] to separate the process contributions in impedance spectra [23]. For each impedance spectrum, the

function dReZ/dLn*f* (where ReZ is the real part of the impedance and *f* is the frequency) was calculated numerically with the data analysis and graphing software OriginPro® 8 (OriginLab). This allows distinguishing more sharply the different electrochemical contributions.

Comparison of performance with dry and humid mixtures: effect of steam

Figure 10 represents the difference between the dReZ/dLn*f* fonctions calculated for the dry and the humid gas mixtures. One major peak is present at 2 Hz, which is independent of temperature but strongly decreases under polarization. A broad shoulder can be observed between 50 and 1000 Hz, which decreases under polarization and is shifted towards higher frequencies as temperature and current are increased. These observations are very similar to those reported by R. Barfod and co-workers [24] in their characterization of an anode supported SOFC with various hydrogen-steam mixtures. According to their analysis, the low-frequency peak is related to the gas conversion, whereas the higher frequency peak is attributed to charge transfer between YSZ and Ni and diffusion of charged species to the triple phase boundary (TPB). They also report a third intermediate peak around 10-100Hz due to gas diffusion. A similar peak can be distinguished here at 860°C in the corresponding frequency range.

Therefore, the initial voltage penalty due to the influence of the excess steam on the Nernst voltage is gradually compensated under polarization by a lower area specific resistance resulting from the facilitated conversion of hydrogen in presence of steam.

Comparison of performance with humid and syngas mixtures: effect of CO/CO_2

Figures 11 and 12 show the impedance spectra measured at respectively 710°C and 860°C under different current biases (OCV, 88, 265 and 442mAcm^{-2}). In accordance with the I-V data, the polarization resistances for the two fuels are similar at 710°C, in particular

at 265 $mAcm^{-2}$ bias. On the contrary, at 860°C, the polarization resistance of the cell with syngas is systematically smaller.

The difference between dReZ/dLn*f* functions calculated for syngas and the humid fuel is shown in Figure 13. Its analysis is not as straight-forward as for the previous case. A low-frequency positive peak can be observed below 1 Hz, which seems to be independent of temperature but diminishes as current is drawn. Two negative peaks are present in the intermediate-frequency range (1-100 Hz). The peak at 6 Hz seems dominant at 710°C but is exceeded by the secondary 40 Hz peak at 810°C. Both peaks are reduced under polarization and increase with temperature. As we are considering the difference (humid-syngas), a positive peak corresponds to additional impedance due to the presence of CO-CO_2 in the fuel. Therefore, the lowest frequency peak (<1 Hz) could be attributed to CO conversion, by analogy to the analysis of the (dry-humid) case. This peak being at a lower frequency compared to the H_2 conversion peak (2 Hz) is consistent with the fact that electrochemical conversion of CO on Ni-YSZ is known to be slower than that of H_2 [25, 26]. Furthermore, this low-frequency peak is negligible at 710°C and becomes significant only above 760°C, indicating that CO is only scarcely electrochemically converted at 710°C.

The intermediate-frequency peaks are more puzzling. Being negative means that they correspond to an improvement compared to the humid H_2 case. Furthermore, this comparative improvement increases with temperature. Intermediate-frequency impedances are often attributed to gas diffusion limited processes [24]. In our case, this is consistent with the fact that the position (frequency) of the peaks is almost not affected by temperature, meaning that the corresponding activation energy is low as for gas diffusion. Matsuzaki and co-workers have shown that, in H_2/CO mixtures, the water-gas shift reaction plays an important role because it is much faster than the oxidation reactions [26].

Therefore, the intermediate peaks could be related to the additional H_2 production through the water-gas shift reaction.

According to these considerations, CO would contribute directly to the electrochemical reaction but in a minor way and also indirectly through the water-gas shift reaction. These contributions are however negligible at low temperature, because of the low fuel utilization conditions reached in this study and the preferential oxidation of H_2. These beneficial contributions become however significant at higher temperatures as the global polarization resistance is reduced, explaining the improved performance of syngas over the humid hydrogen. This however remains speculative and would require additional investigations.

Comparison of performance with syngas and ethanol mixture

Regarding the difference between steam/ethanol and syngas, the impedance spectra measured at 710°C show that the polarization resistance is larger for the internal reforming conditions (Figure 14). At 860°C (Figure 15), the total resistances for both fuels are similar although the polarization resistance remains larger for the steam/ethanol mixture. The latter is however compensated by a reduction of the ohmic resistance, which could originate from an improvement of the contact resistance due to carbon deposition, as suggested by references [11] and [4]. The formation of coke at higher temperatures is also suggested by the significant amount of ethene (7% of the dry gas composition) observed at 780°C in the catalytic test (cf. Figure 3). Ethene is effectively known to form easily coke by decomposition. It is however difficult to know where this carbon deposition occurred. Unfortunately, no post-test examination could be done on the cell because it experienced a fuel shortage during steady-state polarization, which resulted in its failure. After disassembly of the set-up, the internal surface of the fuel inlet quartz cane was covered with coke, which shows that ethanol tends to form coke even at a steam to carbon molar ratio of 1.5 that is supposed to be safe from a thermodynamical point of view. Furthermore,

the gold mesh used for the anode current collection was completely swollen at the fuel inlet, indicating possible coke accumulation between the Ni-rich current collection layer and the mesh. Nevertheless, short-term steady-state polarization at 0.3 Acm^{-2} and 800°C during 20 hours showed no significant voltage degradation. All these observations seem to indicate that coke formation occurred in the Ni-rich anode contact layer but not on the anode active sites. In this case, there is nevertheless a risk of plugging on the long-term.

The difference plot of the dReZ/dLn*f* functions calculated for syngas and ethanol is shown in Figure 16. Here again the trend is quite complex. At 710°C, a series of 3 peaks between 10 and 20'000 Hz and a low-frequency peak around 0.1 Hz can be distinguished. At 760, 810°C, the picture is more confused and at 860°C, the peaks have almost vanished except the low-frequency peak. At 710°C, we can basically distinguish peaks around 100, 1'000 and 10'000 Hz. The 100 and 1'000 Hz peaks are reduced under polarization, whereas the 10 kHz peak is independent of the current bias. The catalytic ethanol steam reforming measurements performed separately on crushed Ni-YSZ anode support powder have revealed the presence of more methane and ethene in the reformate gas (respectively 7-10% and 4-7% of the dry gas composition) than predicted by thermodynamic calculation, especially above 700°C (cf. Fig. 3 and 4). In their study of internal reforming of methane on Ni-YSZ anode, Bebelis and co-workers [27] observed at OCV a principal peak around 1kHz and a small peak around 0.1 Hz. They observed a reduction of the amplitude of the peaks with increasing temperature and bias, and a shift of the 1kHz peak towards higher frequencies with increasing polarization. These trends can also be observed for the 1kHz peak in Figure 16, particularly at 760 and 810°C. The peaks in Fig. 16 could therefore be attributed to the presence of methane and ethene in the internally reformed steam/ethanol mixture.

A more refined analysis of the impedance spectra using equivalent circuits would be necessary to get a better understanding of the limiting mechanisms ruling internal ethanol

steam reforming on Ni-YSZ. However, the electrochemical performance of Ni-YSZ is strongly influenced by its catalytic properties: at low temperature, where ethanol is only partially reformed, the performance is poor, whereas above 800°C, where ethanol is catalytically almost fully reformed, the performance is improved by the direct and the indirect conversion of CO. The possible presence of methane and ethene increases the polarization losses and is accompanied by carbon deposition.

Conclusions

Internal ethanol steam reforming on a standard Ni-YSZ anode supported solid oxide fuel cell was investigated by comparing the electrochemical performance of the cell with different fuels: steam/ethanol, its corresponding reformate gas, humidified hydrogen and dry hydrogen. Electrochemical impedance spectroscopy was further used to get a better insight of the limiting mechanisms.

It was shown that the electrochemical performance of standard Ni-YSZ anode for the internal steam reforming of ethanol is directly related to the catalytic conversion of ethanol, i.e. to the availability of H_2. At 700°C, the latter is only 30% and therefore, the electrochemical performance is poor compared to that obtained with the reformate gas. At 780°C, it reaches 80% and the electrochemical performance is similar to that obtained with the reformate gas.

Comparison between the performances obtained with humid H_2 and reformate gas indicates that CO contributes to the electrochemical reaction on Ni-YSZ only above 760°C and mainly through the water-gas shift reaction, at least under low fuel utilization testing conditions.

Carbon deposition above 760°C was suspected because of the sudden reduction of the cell's contact resistance with steam/ethanol (3 to 1 molar) and attributed to the decomposition of ethene.

Additional polarization losses were observed with steam/ethanol feed and attributed to the presence of methane and ethene resulting from the internal steam reforming of ethanol on the anode material. Ni-YSZ seems to operate well under fully reformed ethanol and should therefore be coupled with a better reforming catalyst less sensitive to carbon deposition.

The results presented in this study should be considered as preliminary: the impedance spectra obtained with the different fuels still have to be analyzed in more detail using equivalent circuits in order to elude the limiting mechanisms. This study on standard Ni-YSZ will nevertheless be used as a benchmark for the characterization of improved anode materials.

Acknowledgments

This work was supported by the Swiss State Secretariat for Education and Research (SER) (contract Nr SER C08.0127) within the framework of COST action 543. HTceramix is acknowledged for providing the anode supported electrolyte half cells.

References

[1] P. Tsiakaras, A. Demin, Journal of Power Sources, 102 (2001) 210-217.
[2] G.J. Saunders, K. Kendall, Journal of Power Sources, 106 (2002) 258-263.
[3] G.J. Saunders, J. Preece, K. Kendall, Journal of Power Sources, 131 (2004) 23-26.
[4] M. Cimenti, J.M. Hill, Journal of Power Sources, 195 3996-4001.
[5] X.F. Ye, S.R. Wang, Q. Hu, Z.R. Wang, T.L. Wen, Z.Y. Wen, Electrochemistry Communications, 11 (2009) 823-826.
[6] X.F. Ye, S.R. Wang, Q. Hu, J.Y. Chen, T.L. Wen, Z.Y. Wen, Solid State Ionics, 180 (2009) 276-281.
[7] X.F. Ye, S.R. Wang, Z.R. Wang, Q. Hu, X.F. Sun, T.L. Wen, Z.Y. Wen, Journal of Power Sources, 183 (2008) 512-517.

[8] S.A. Venancio, T.F. Gutierres, B.J.M. Sarruf, P.E.V. Miranda, Materia-Rio De Janeiro, 13 (2008) 560-568.
[9] R. Muccillo, E.N.S. Muccillo, F.C. Fonseca, D.Z. de Florio, Journal of the Electrochemical Society, 155 (2008) B232-B235.
[10] M. Yano, T. Kawai, K. Okamoto, M. Nagao, M. Sano, A. Tomita, T. Hibino, Journal of the Electrochemical society 154 (2007) B865–B870.
[11] B. Huang, S.R. Wang, R.Z. Liu, T.L. Wen, Journal of Power Sources, 167 (2007) 288-294.
[12] Y. Jiang, A.V. Virkar, Journal of the Electrochemical Society, 148 (2001) A706-A709.
[13] B. Huang, S.R. Wang, R.Z. Liu, X.E. Ye, H.W. Nie, X.E. Sun, T.L. Wen, Journal of Power Sources, 167 (2007) 39-46.
[14] K. Sasaki, K. Watanabe, Y. Teraoka, Journal of the Electrochemical Society, 151 (2004) A965-A970.
[15] X.F. Ye, B. Huang, S.R. Wang, Z.R. Wang, L. Xiong, T.L. Wen, Journal of Power Sources, 164 (2007) 203-209.
[16] B. Zhu, Journal of Power Sources, 93 (2001) 82-86.
[17] B. Huang, X.J. Zhu, W.Q. Hu, Y.Y. Wang, Q.C. Yu, Journal of Power Sources, 195 3053-3059.
[18] B. Huang, X.J. Zu, W.Q. Hu, Q.C. Yu, H.Y. Tu, Journal of Power Sources, 186 (2009) 29-36.
[19] A. Arpornwichanop, N. Chalermpanchai, Y. Patcharavorachot, S. Assabumrungrat, M. Tade, International Journal of Hydrogen Energy, 34 (2009) 7780-7788.
[20] H.P. He, J.M. Vohs, R.J. Gorte, Journal of the Electrochemical Society, 150 (2003) A1470-A1475.
[21] P. Tanasini, M. Cannarozzo, P. Costamagna, A. Faes, J. Van Herle, A. Hessler-Wyser, C. Comninellis, Fuel Cells, 9 (2009) 740-752.
[22] S.H. Jensen, A. Hauch, P.V. Hendriksen, M. Mogensen, N. Bonanos, T. Jacobsen, Journal of the Electrochemical Society, 154 (2007) B1325-B1330.
[23] Z. Wuillemin, A. Nakajo, A. MÃ¼ller, A.J. SchÃ¼ler, S. Diethelm, J. Van Herle, D. Favrat, in: ECS Transactions, 2009, pp. 457-466.
[24] R. Barfod, M. Mogensen, T. Klemenso, A. Hagen, Y.L. Liu, P.V. Hendriksen, Journal of the Electrochemical Society, 154 (2007) B371-B378.
[25] R.J. Aaberg, R. Tunold, S. Tjelle, R. Odegard, High Temperature Electrochemistry: Ceramics and Metals, (1996) 511-518.
[26] Y. Matsuzaki, I. Yasuda, Journal of the Electrochemical Society, 147 (2000) 1630-1635.
[27] S. Bebelis, S. Neophytides, Solid State Ionics, 152 (2002) 447-453.

Table 1: gas compositions (%) used for the characterization of the cell

Gas mixture	*H_2*	*H_2O*	*CO*	*CO_2*	*Ar*
Dry	56	-	-	-	44
Humid	56	20	-	-	24
Syngas	56	20	18	6	-

Table 2: Comparison between measured OCVs and calculated Nerst voltage for the humid gas mixture and etOH-steam mixture

T / °C ± 5	*Humid*		*etOH*	
	OCV / mV	Nernst / mV	OCV / mV	Nernst / mV
710	1007	1011	1003	1017
760	989	998	1001	1002
810	975	985	972	989
860	963	971	968	975

Figure captions

Figure 1: Schematic representation of the catalysis set-up

Figure 2: a) Schematic representation of the cell assembly in the Probostat™. b) Picture (by courtesy of NorECs)

Figure 3: Ethanol conversion and dry gas composition obtained from ethanol steam reforming on crushed Ni-YSZ anode support

Figure 4: Thermodynamic dry gas composition for a steam:ethanol 3 to 1 molar ratio.

Figure 5: I-V curves for different gas mixtures feed (cf. Table 1) at 710°C.

Figure 6: I-V curves for different gas mixtures feed (cf. Table 1) at 760°C.

Figure 7: I-V curves for different gas mixtures feed (cf. Table 1) at 810°C.

Figure 8: I-V curves for different gas mixtures feed (cf. Table 1) at 860°C.

Figure 9: Power densities measured at 0.7 V for different gas feeds (cf. Table 1) as a function of temperature.

Figure 10: Difference between the dReZ/dLn*f* functions calculated for the dry and the humid gas mixtures (d-h) at various temperatures.

Figure 11: Comparison of impedance spectra obtained for humid (h) gas mixture and syngas (s) (cf. Table 1) under various DC bias at 710°C.

Figure 12: Comparison of impedance spectra obtained for humid (h) gas mixture and syngas (s) (cf. Table 1) under various DC bias at 860°C.

Figure 13: Difference between the dReZ/dLn*f* functions calculated for the humid gas mixture and the syngas (h-s) at various temperatures.

Figure 14: Comparison of impedance spectra obtained for humid syngas (s) and steam/ethanol (e) (cf. Table 1) under various DC bias at 710°C.

Figure 15: Comparison of impedance spectra obtained for syngas (s) and steam/ethanol (e) (cf. Table 1) under various DC bias at 860°C.

Figure 16: Difference between the dReZ/dLn*f* functions calculated for the syngas and the steam/ethanol (s-e) at various temperatures.

Figure 1

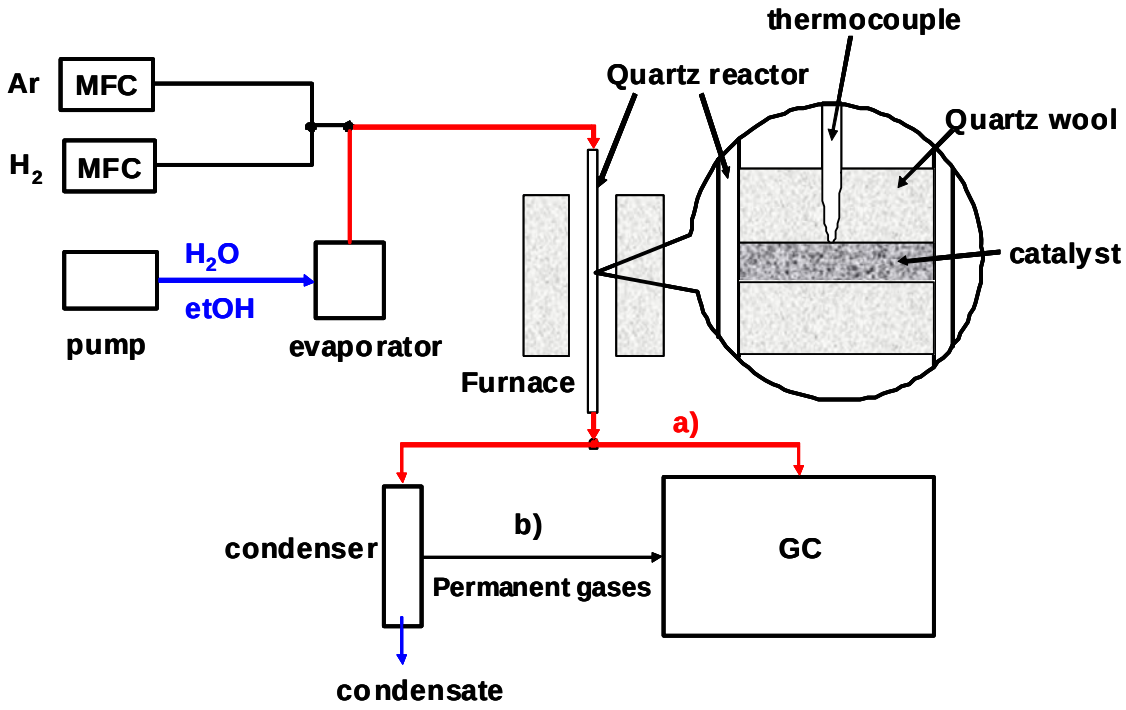

Figure 2

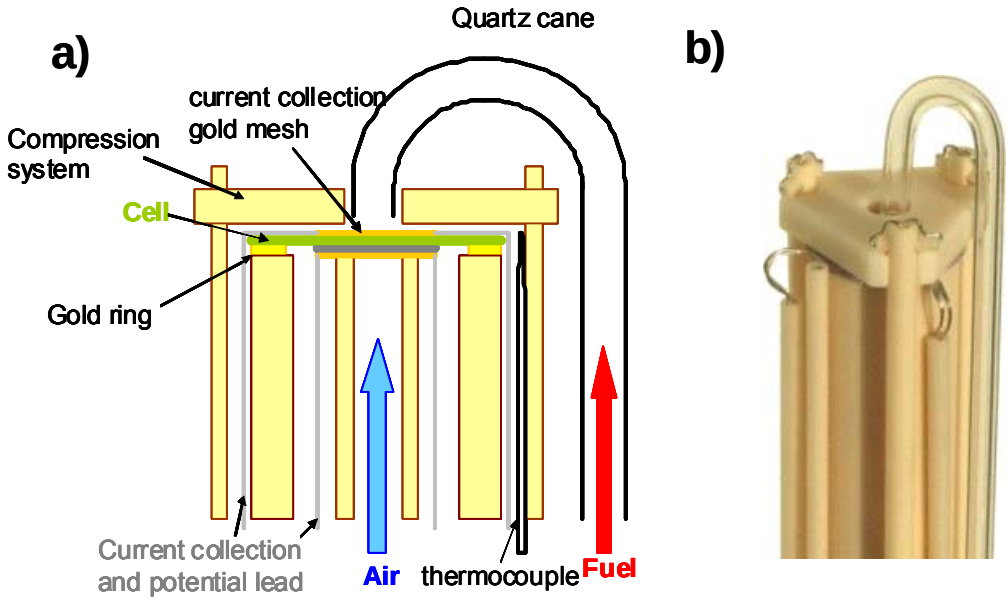

Figure 3

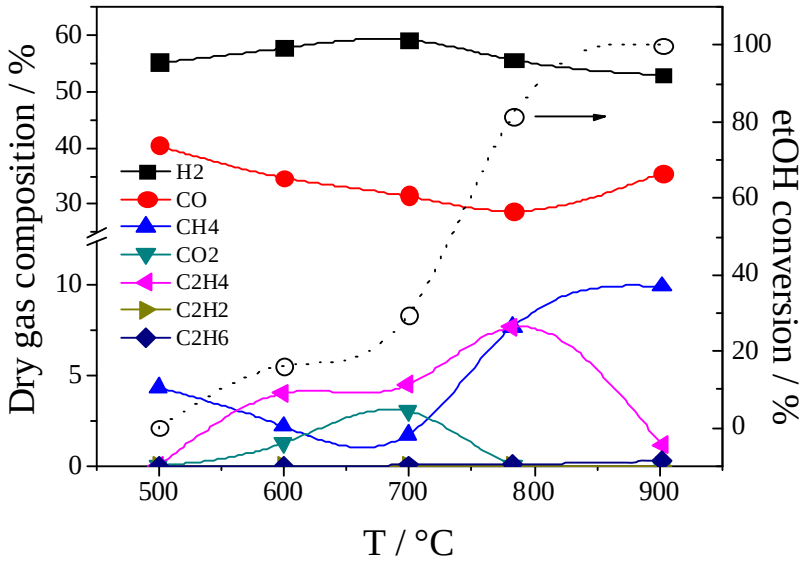

Figure 4

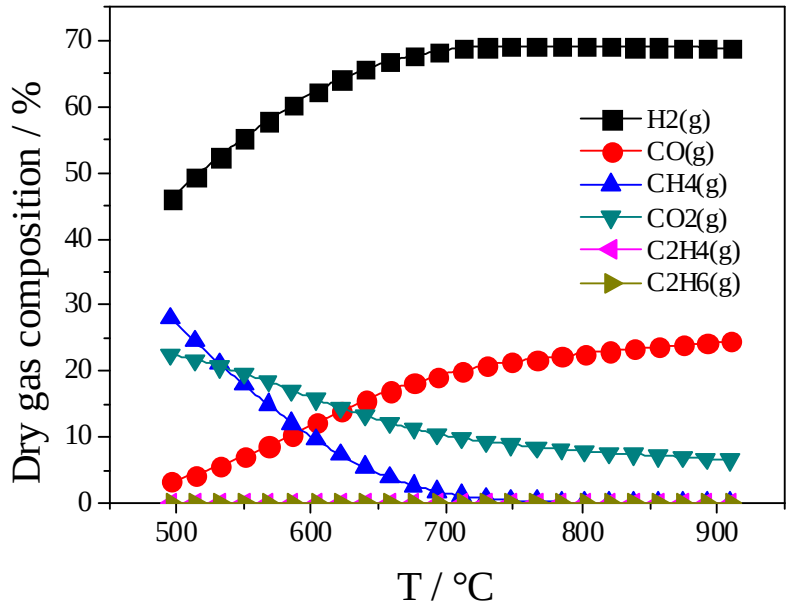

Figure 5

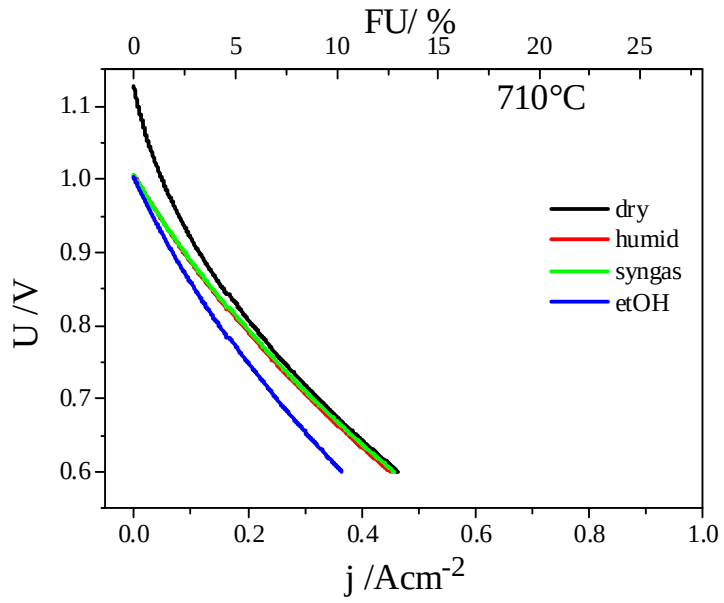

Figure 6

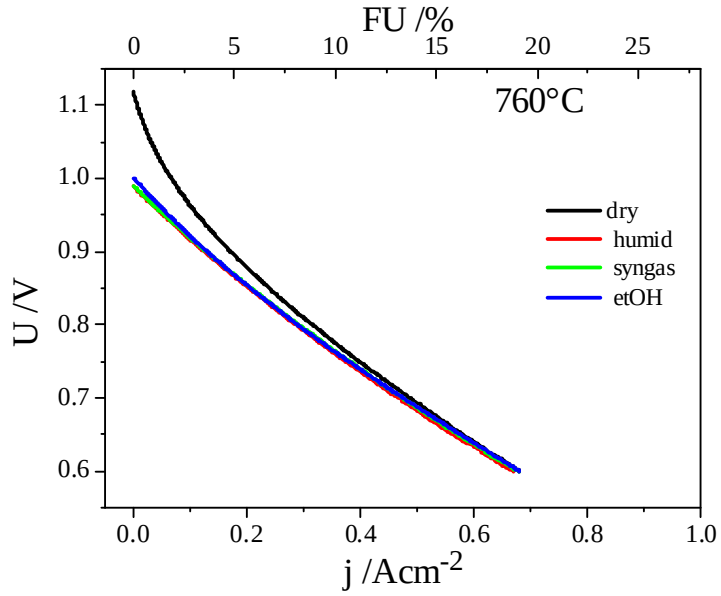

Figure 7

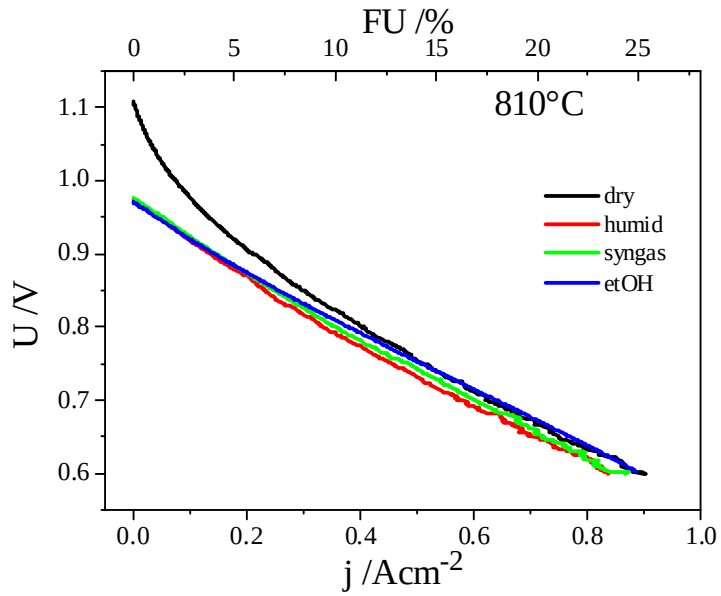

Figure 8

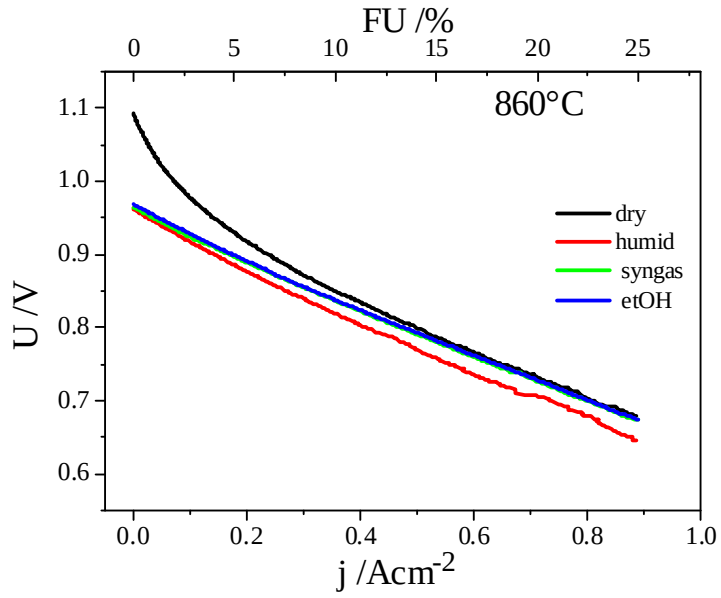

Figure 9

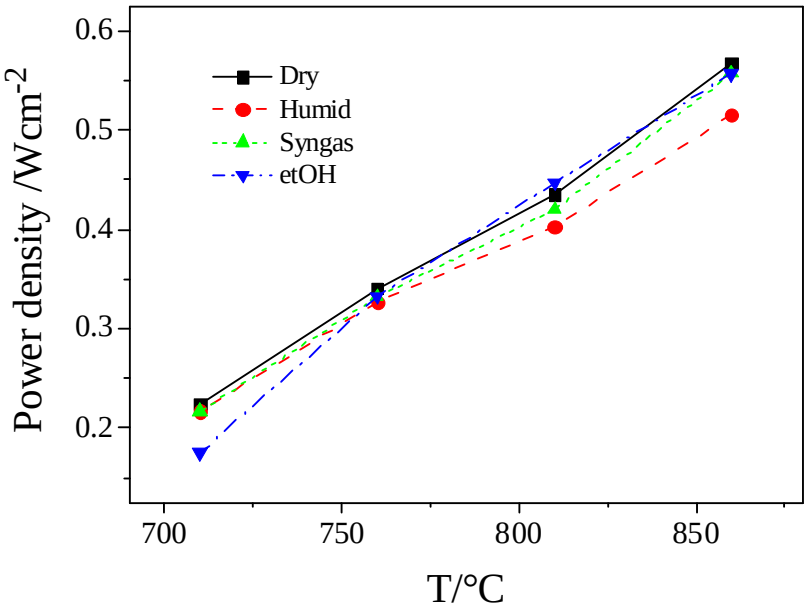

Figure 10

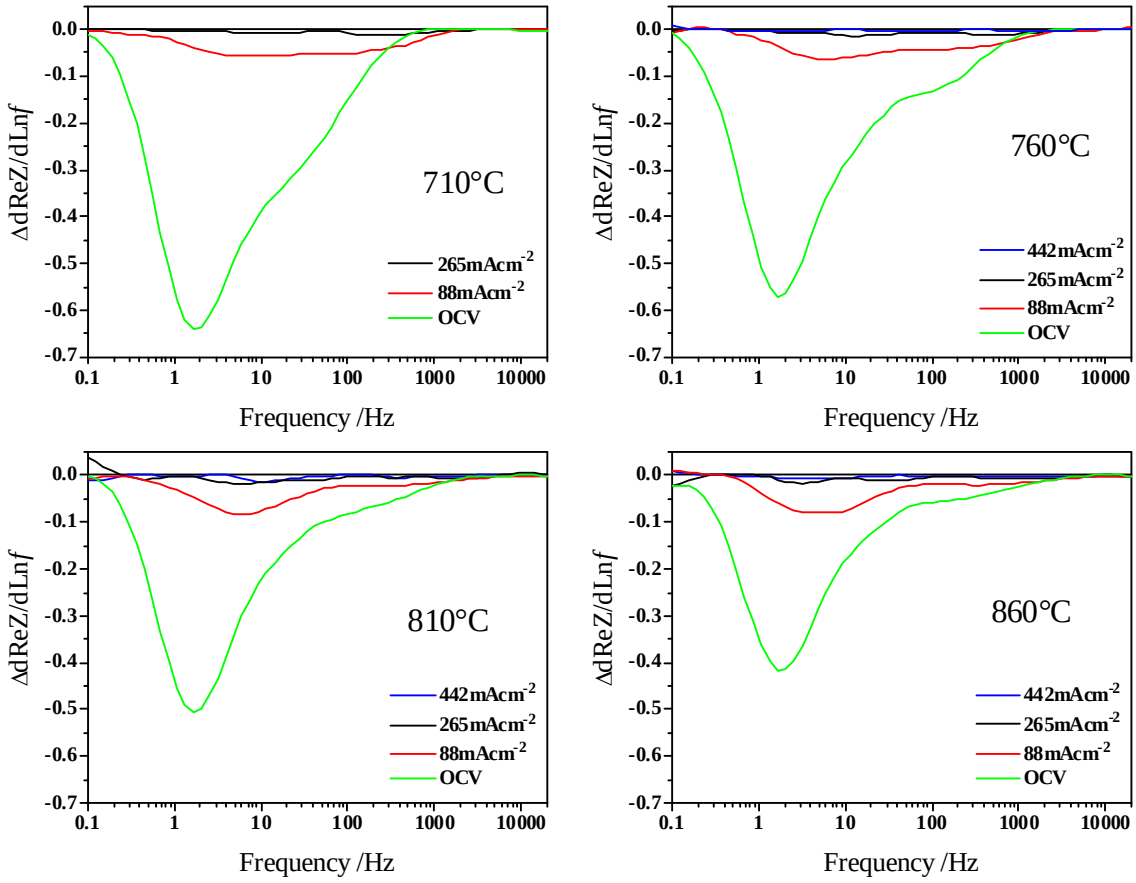

Figure 11

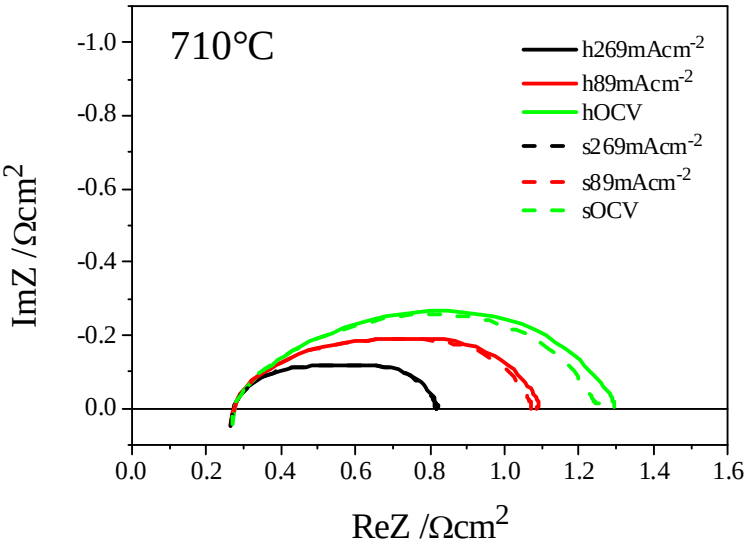

Figure 12

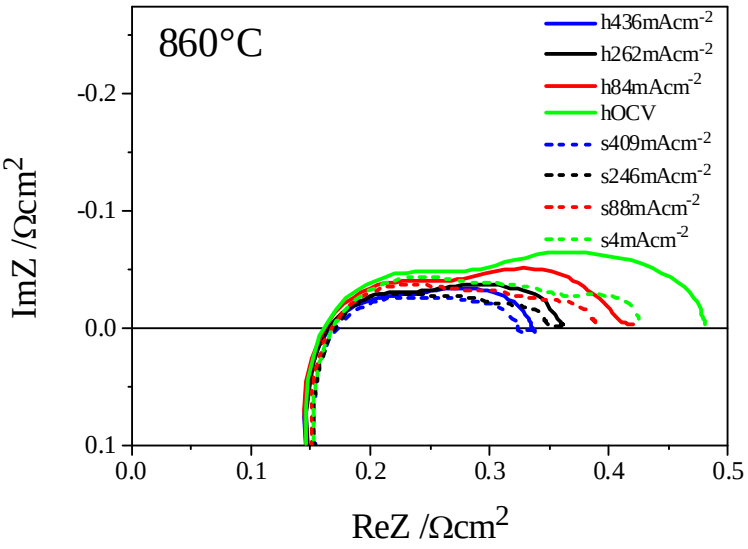

Figure 13

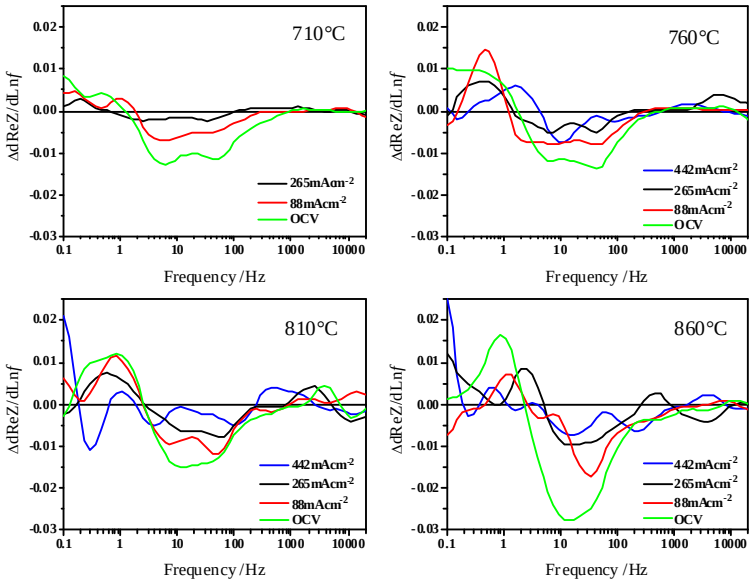

Figure 14

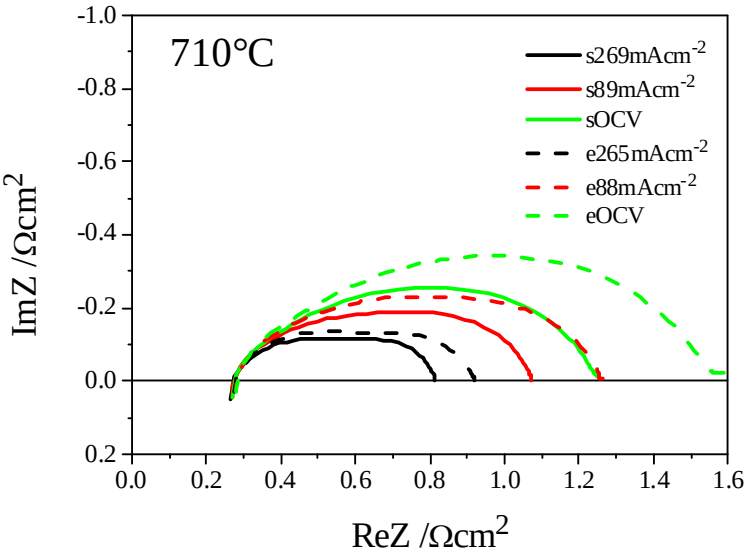

Figure 15

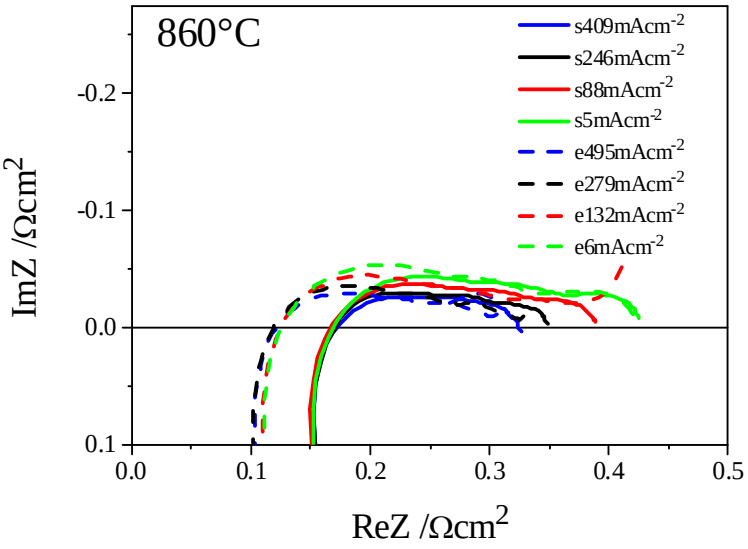

Figure 16